


## RESEARCH ARTICLE

# Sclareol ameliorates hyperglycemia-induced renal injury through inhibiting the MAPK/NF- $\kappa$ B signaling pathway

Xue Han<sup>1,2</sup> | Jiajia Zhang<sup>1</sup> | Li Zhou<sup>3</sup> | Jiajia Wei<sup>2</sup> | Yu Tu<sup>2</sup> | Qiaojuan Shi<sup>2</sup> | Yi Zhang<sup>1</sup> | Juan Ren<sup>1</sup> | Yi Wang<sup>4</sup> | Huazhong Ying<sup>1,3</sup> | Guang Liang<sup>2,4</sup> 

<sup>1</sup>Zhejiang Provincial Key Laboratory of Laboratory Animals and Safety Research, Hangzhou Medical College, Hangzhou, China

<sup>2</sup>School of Pharmaceutical Sciences, Hangzhou Medical College, Hangzhou, China

<sup>3</sup>College of Pharmaceutical Science, Zhejiang Chinese Medical University, Hangzhou, China

<sup>4</sup>Chemical Biology Research Center, School of Pharmaceutical Sciences, Wenzhou Medical University, Wenzhou, China

## Correspondence

Huazhong Ying, Zhejiang Provincial Key Laboratory of Laboratory Animals and Safety Research, Hangzhou Medical College, 182 Tianmushan Road, Hangzhou, Zhejiang 310013, China.

Email: [yhz0101@126.com](mailto:yhz0101@126.com)

Guang Liang, School of Pharmaceutical Sciences, Hangzhou Medical College, 182 Tianmushan Road, Hangzhou, Zhejiang 310013, China.

Email: [wzmcliangguang@163.com](mailto:wzmcliangguang@163.com)

## Funding information

National Natural Science Foundation of China, Grant/Award Numbers: 21961142009, 31900381; the Basic Scientific Research Project of Hangzhou Medical College, Grant/Award Numbers: KYB202114, KYZD202102; the Natural Science Foundation of Zhejiang Province, Grant/Award Number: LGJ18H310002; Wenzhou Science and Technology Key Project, Grant/Award Number: 2018ZY009; Zhejiang Provincial Key Scientific Project, Grant/Award Number: 2021C03041

## Abstract

Diabetic nephropathy (DN) represents the most serious complication of diabetes. Previous studies have shown that the activation of nuclear factor kappa B (NF- $\kappa$ B) and mitogen-activated protein kinase (MAPK) are linked to inflammation in the development of DN. Sclareol, a natural diterpene compound, has beneficial effects on inflammation. Thus, we hypothesized that sclareol might prevent DN via anti-inflammatory actions. This study aimed to investigate the actions of sclareol in the progression of DN, and explored the related molecular mechanism. Sclareol treatment significantly alleviated renal dysfunction, fibrosis, and inflammatory cytokine levels in a dose-dependent manner in diabetic mice. Moreover, sclareol inhibited the activations of MAPKs and NF- $\kappa$ B in diabetic kidney tissues. The therapeutic effects of sclareol were confirmed under high levels of glucose in SV40 cells, and sclareol prevented high glucose-induced fibrosis and inflammatory responses, which was largely driven by MAPKs and NF- $\kappa$ B inhibitions. In particular, MAPKs inhibitors mixture could suppress the NF- $\kappa$ B pathway and release of inflammatory cytokines that sclareol was involved in. In conclusion, sclareol has benefits for diabetes-induced renal dysfunction, which was partially associated with amelioration of fibrosis and inflammation via mediation of the MAPK/NF- $\kappa$ B signaling pathway. Sclareol may be a promising agent for preventing the progression of DN.

## KEYWORDS

diabetic nephropathy, inflammation, mitogen-activated protein kinase, nuclear factor kappa B, sclareol

## 1 | INTRODUCTION

Diabetes mellitus (DM) has become an extensive health problem with a high risk of intractable complications (Kale, Sankrityayan, Anders, & Gaikwad, 2021). Diabetic nephropathy (DN) is one of the most feared complications of both type 1 DM (T1DM) and type 2 DM (T2DM),

given that it influences nearly 30% of patients with DM (Fioretto, Zambon, Rossato, Busetto, & Vettor, 2016). Indeed, DN is well known as the root cause of end-stage renal disease (ESRD). Major risk factors for DN include hyperglycemia, hypertension, hyperlipidemia, obesity, and smoking (Jaimes et al., 2021). Known clinical management for DN is directed at tight glycemic control, blood pressure lowering, and hypolipidemic agents. These treatment strategies can only slow the development of DN but cannot reliably prevent the progression to

Xue Han and Jiajia Zhang contributed equally to this work.

ESRD (Varma, Kajdacsy-Balla, Akkina, Setty, & Walsh, 2016). Therefore, there remains a need to discover novel agents for the treatment of DN.

Several studies have shown the beneficial effects of natural compounds in DN treatments (Kumar, Mittal, Babu, & Mittal, 2021). Sclareol, a kind of labdane-type diterpene, is isolated from *Salvia sclarea*, which is widely used in food industries, folk medicine, and cosmetics (Zhang, Wang, & Cai, 2017). Popularly known, sclareol possesses renowned bioactive properties, such as anticancer, antioxidant, and anti-inflammatory effects (Duan, Hou, Ji, & Deng, 2018; Ravera et al., 2020; Tsai et al., 2018). Studies have reported that this diterpene relieves the severity of rheumatoid arthritis by modulating excessive inflammation in mice (Tsai et al., 2018). In addition, in view of the metabolic benefits of sclareol, it has been reported to improve the metabolic profile of obese mice in multiple aspects, including insulin sensitivity, glucose tolerance, and adiposity (Cerri et al., 2019). However, the role of sclareol on DN, and its possible use for the treatment of DN are still unknown.

Although several potential mechanisms have been implicated in the development of DN, the chronic inflammatory state created by hyperglycemia is perhaps the most consequential (Patel, Bose, & Cooper, 2020). Microinflammation contributes to glomerular endothelial cell injuries, together with upregulation of adhesion molecules and chemokines, which lead to macrophage infiltration into renal tissues (Wada & Makino, 2013). Mitogen-activated protein kinases (MAPKs) can be activated by various stimuli, including inflammation. There is strong evidence supporting the key role of MAPKs in the pathogenesis of DN, as an increase in the phosphorylation of MAPKs has been measured in the kidney tissues of diabetic mice (Jiao et al., 2015). Nuclear factor-kappa B (NF- $\kappa$ B) serves as a crucial factor in modulating inflammation in DN that can be activated by MAPK (Kang et al., 2017). The active form of NF- $\kappa$ B has been shown to upregulate the transcription of inflammatory cytokines such as tumor necrosis factor- $\alpha$  (TNF- $\alpha$ ), interleukin-6 (IL-6), and IL-1 $\beta$  (Mozzini, Cominacini, Garbin, & Fratta Pasini, 2017). These proinflammatory factors are major contributors to renal fibrosis, as they promote extracellular matrix deposition and renal dysfunction through feedback activation of signaling pathways such as MAPK and NF- $\kappa$ B pathways (Ravera et al., 2020). Therefore, a hyperglycemia-induced inflammatory response may represent a promising direction of intervention to halt DN progression. It has been reported that sclareol protects against bone loss by suppressing MAPK and NF- $\kappa$ B pathway activation (Jin et al., 2019). Based on the above promising results, we hypothesize that sclareol protects against diabetes-induced kidney injury via the inhibition of MAPK and NF- $\kappa$ B-mediated inflammation in mice.

Thus, this study aimed to explore the pharmacological effect of sclareol against DN in streptozotocin (STZ)-induced type I diabetic mice. We further confirmed these results in glomerular mesangial cells stimulated by high level of glucose. We found that sclareol treatment suppressed diabetes-induced renal inflammation and fibrosis both in vivo and in vitro, which was mediated by the ability to inhibit

MAPKs and NF- $\kappa$ B activation. In summary, our study identified NF- $\kappa$ B as a new candidate for the treatment of DN.

## 2 | MATERIALS AND METHODS

### 2.1 | Animals

Male C57BL/6 mice (weight  $20 \pm 2$  g) were obtained from the Laboratory Animal Center of Hangzhou Medical College (Hangzhou, China). All mice were housed in a habitant at 23–26°C, 40%–60% humidity, and with a 12 hr light–dark cycle. Mice were allowed free access to food and water. Experimental procedures were performed according to the National Institutes of Health Guidelines for the Care and Use of Laboratory Animals. Animal care and experimental protocols were approved by the Ethics Committee of Laboratory Animal Care and Welfare, Hangzhou Medical College, with the Approval Number 2021-138.

### 2.2 | Mice model of type I diabetic mice

To induce the type I diabetic mice model, mice were intraperitoneally injected with STZ (Sigma-Aldrich, MO, USA) in a single injection. The dose of STZ was 100 mg/kg which has been reported to reliably induce T1DM in mice (Wang et al., 2020). STZ was dissolved in 0.1 M sodium citrate buffer (pH 4.5). Age-matched mice received citrate buffer and served as the control group. All mice received common food (Zhejiang Academy of Medical Sciences, Hangzhou, China) during experiment. The concentration of fasting blood-glucose was measured using a glucometer once a week. Mice with fasting blood-glucose  $\geq 12$  mmol/L were regarded as diabetic mice and used for subsequent experiments. On the ninth week, the compound treatment was initiated, and the diabetic mice were randomly divided into three experimental groups ( $n = 6$  per group): vehicle group (0.5% CMC-Na solution, *i.g.*), low-dose sclareol group (5 mg/kg, *i.g.*; the chemical structure was shown in Figure 1a; purity, 98.5%; Shanghai yuanye Bio-Technology Co., Ltd, Shanghai, China), and high-dose sclareol group (10 mg/kg, *i.g.*). Sclareol was administered every day for 5 weeks. The vehicle group received the CMC-Na solution following the same schedule. The dose of sclareol was chosen according to a previous report with minor modifications (Jin et al., 2019). Blood glucose and body weight were monitored every week. At the end of the study, the mice were anesthetized with phenobarbital sodium (40 mg/kg, *i.p.*). Blood and kidney tissues were collected (Figure 1b). Levels of blood urea nitrogen (BUN), urine creatinine and albumin were measured using a commercial assay (Jiancheng, Jiangsu, China).

### 2.3 | Kidney staining

Kidney tissues were fixed with 4% paraformaldehyde at room temperature for 48 hr, and then embedded in paraffin. The samples were



Primer sequences for TNF- $\alpha$ , IL-6, IL-1 $\beta$ , collagen IV (col-4), transforming growth factor beta (TGF- $\beta$ ), intercellular cell adhesion molecule-1 (ICAM-1), vascular cellular adhesion molecule-1 (VCAM-1), monocyte chemoattractant protein-1 (MCP-1), and  $\beta$ -actin were synthesized in Sangon Biotech (Shanghai, China) as listed in the Table S1. The relative amount was normalized to that of  $\beta$ -actin.

## 2.5 | Preparation of cell culture

The mouse glomerular mesangial cell line SV40 MES-13 was bought from the Shanghai Institute of Biochemistry and Cell Biology (Shanghai, China). Cells were cultured in Dulbecco's Modified Eagle's Medium (DMEM; Gibco, Eggenstein, Germany) that contained 5.5 mM of D-glucose with 10% fetal bovine serum (FBS; Hyclone, UT, USA), 100 U/ml of penicillin, and 100 mg/ml of streptomycin. Cells were incubated at 37°C with 5% CO<sub>2</sub>. In cellular experiments, SV40 MES-13 cells were pretreated with sclareol (10  $\mu$ M and 20  $\mu$ M) or with MAPK inhibitors mixture (JNK inhibitor, SP600125, 5  $\mu$ M; ERK inhibitor, U0126, 5  $\mu$ M; p38 inhibitor, SB230580, 5  $\mu$ M; Sigma, MO, United States) for 1 hr. The DMEM containing 5.5 mM glucose (normal glucose, NG) was regarded as control, and DMEM containing 27.5 mM D-glucose (Sigma; total 33 mM) was served as high glucose (HG) group. In addition, DMEM containing 27.5 mM mannitol was served as an osmotic control.

## 2.6 | Cell viability assay

SV40 MES-13 cells (Shanghai Institute of Biochemistry and Cell Biology, Shanghai, China; passage 5) were planted in 96-well plates at 5,000 cells per well and cultured overnight for adherence. Cells were exposed to sclareol (dissolved in DMSO) in the following concentrations: 3.125, 6.25, 12.5, 25, 50, 100, and 200  $\mu$ M. Cell viability was detected using a cell counting kit-8 assay (CCK-8; Dojindo Laboratory, Kumamoto, Japan) according to the manufacturer's instructions. After 24 hr of culturing, cells were washed with PBS and incubated in DMEM containing 10  $\mu$ l of CCK-8 solution for 30 min at 37°C. The optical density was determined at 450 nm using a Microplate Reader (Bio-Rad).

## 2.7 | Immunofluorescence assay

To observe the nuclear localization of NF- $\kappa$ B p65, an immunofluorescence assay was applied. SV40 MES-13 cells were planted into a 6-well plate. Following the agent treatment, cells were fixed with 4% paraformaldehyde and permeabilized with 0.1% Triton X-100. Cells were then stained with anti-NF- $\kappa$ B p65 antibody (Cat. NO. 10745-1-AP, 1:300; Proteintech, Wuhan, China) overnight at 4°C. Phycoerythrin-conjugated secondary antibody was incubated for 2 hr at room temperature. Cell nuclei were counterstained with DAPI. Images were taken with a confocal microscope (A1R-SIM-STORM, Nikon, Japan).

## 2.8 | Western blot analysis

The whole proteins were isolated using a cell and tissue total protein extraction kit (Cat. NO. KC415, Kang Cheng Bioengineering Co., Ltd., Shanghai, China), while the cytosolic and nuclear proteins were isolated using a nuclear and cytoplasmic protein extraction kit (cat. NO. P0028, Beyotime Biotechnology, Shanghai, China). Protein samples were measured with a BCA protein assay kit (cat. NO. P0010, Beyotime). Proteins were separated with SDS-PAGE gels and electrotransferred to polyvinylidene fluoride membranes. After blocking with 5% non-fat milk or 5% BSA at room temperature for 1 hr, the membranes were incubated overnight at 4°C with various primary antibodies. Antibodies for phospho-JNK (Cat. NO. 9255, 1:1000), JNK (Cat. NO. 9252, 1:1000), and phospho-p38 (Cat. NO. 4511, 1:1000) were obtained from Cell Signaling Technology (USA). Antibodies for p38 (Cat. NO. 14064-1-AP, 1:1000), phospho-ERK1/2 (Cat. NO. 28733-1-AP, 1:1000), ERK1/2 (cat. NO. 16433-1-AP, 1:1000), NF- $\kappa$ B p65 (Cat. NO. 10745-1-AP, 1:1000), I $\kappa$ B (Cat. NO. 10268-1-AP, 1:1000), Lamin B (Cat. NO. 66095-1-Ig, 1:1000) and GAPDH (Cat. NO. 60004-1-Ig, 1:1000) were purchased from Proteintech (China). HRP-conjugated secondary antibodies (1:3000, Servicebio, China) were applied for 2 h at room temperature. Specific bands were detected using the ECL chemiluminescence kit. The band density was processed and quantified with ImageJ software (NIH, Bethesda, MD, USA). Either GAPDH or Lamin B served as the internal control.

## 2.9 | Statistical analysis

All experiments were randomized and blinded. Data were expressed as mean  $\pm$  SEM from at least three independent experiments. All statistical analyses were performed using GraphPad Pro Prism 8.01 (GraphPad, CA, USA). One-way ANOVA followed by a multiple comparisons test with Tukey was used to analyze the differences.  $p < 0.05$  was considered significant.

## 3 | RESULTS

### 3.1 | Sclareol attenuates diabetes-induced renal dysfunction

To investigate whether sclareol treatment has a protective effect against the development of diabetic nephropathy, we established an STZ-induced type I diabetic mouse model through the daily administration of 5g or 10 mg/kg of sclareol for 5 weeks. As expected, diabetic mice exhibited increased blood glucose concentrations and decreased body weight gains compared with control mice (Figure 1c and d), while there were no differences among sclareol treatment groups and the T1DM group. Diabetic mice also showed elevated kidney to body weight ratios, BUN content, and urine albumin to creatinine levels ( $p < 0.001$ , Figure 1e-g). Sclareol treatment dose-dependently corrected these changes, indicating that sclareol attenuated kidney dysfunction in diabetic mice ( $p < 0.05$ ).

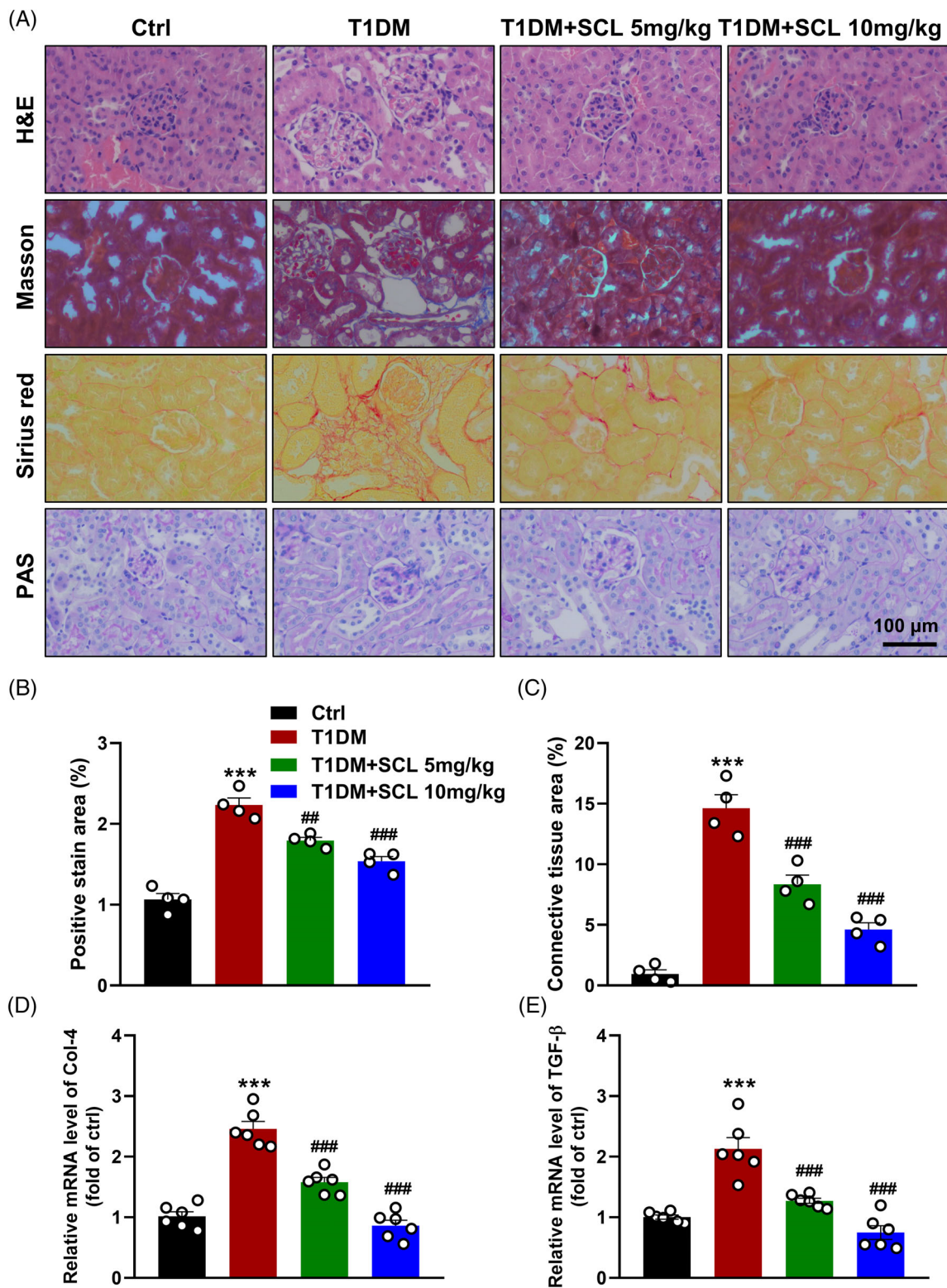


**FIGURE 2** Sclerol normalizes diabetes-induced renal fibrosis. (a) Representative images of H&E, Masson's Trichrome, Sirius Red, and Periodic acid-Schiff in kidney tissues. Scale bar, 100  $\mu$ m. Quantification analysis of Masson staining (b) and Sirius red staining (c). RT-PCR analysis of transcript levels of col-4 (d) and TGF- $\beta$  (e) in kidney tissues. Values are mean  $\pm$  SD, (a-c:  $n = 4$  per group; d, e:  $n = 6$  per group). \*\*\* $p < 0.001$  versus ctrl; ## $p < 0.01$ , ### $p < 0.001$  versus T1DM. Ctrl, control; T1DM, type 1 diabetes mellitus

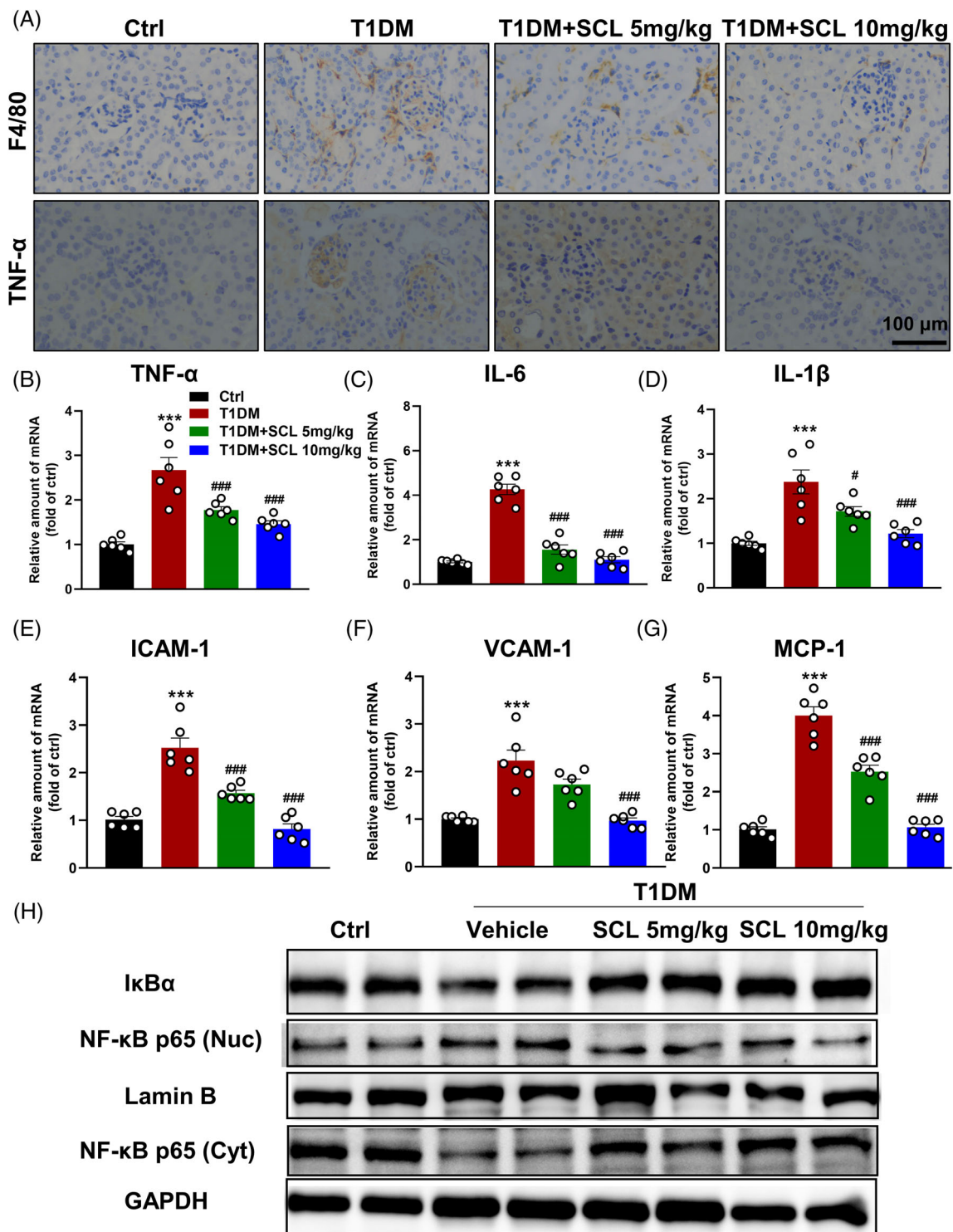


**FIGURE 3** Scleareol prevents diabetes-induced inflammatory response in kidneys by inhibiting NF- $\kappa$ B pathway. (a) Representative images of immunohistochemical staining for F4/80 and TNF- $\alpha$ . Scale bar, 100  $\mu$ m. Transcript levels of TNF- $\alpha$  (b), IL-6 (c), IL-1 $\beta$  (d), ICAM-1 (e), VCAM-1 (f), and MCP-1 (g) were measured with RT-PCR in kidney tissues. (h) Western blot assay was used to detect protein levels of NF- $\kappa$ B pathway. Values are mean  $\pm$  SD, (b–g:  $n = 6$  per group; H:  $n = 4$  per group). \*\*\* $p < 0.001$  versus ctrl; # $p < 0.05$ , ### $p < 0.001$  versus T1DM. Ctrl, control; T1DM, type 1 diabetes mellitus

### 3.2 | Sclareol normalizes diabetes-induced renal fibrosis

We performed pathological assessments and quantitative polymerase chain reaction (qPCR) of fibrosis indexes in kidneys to evaluate whether sclareol is involved in protecting against renal fibrosis. H&E staining of T1DM mouse kidneys showed glomerulosclerosis, mesangial cells, and matrix expansion (Figure 2a). Masson's trichrome staining and Sirius red staining showed elevated fibrosis and interstitial collagen deposition in the diabetic kidney tissues ( $p < 0.001$ , Figure 2a–c). PAS staining has been reported to negatively correlate with kidney function (Vleming et al., 1997). PAS-positive material was clearly shown in kidney specimens from T1DM mice. Sclareol at both 5 and 10 mg/kg normalized these diabetes-associated pathological changes including structural development, fibrosis, and collagen deposition in kidney tissues (Figure 2a–c). In addition, transcript levels of col-4 and TGF- $\beta$  were significantly increased in kidney samples from T1DM mice when compared to control mice ( $p < 0.001$ , Figure 2d,e). None of the mRNA measures showed increases in kidney tissues from T1DM mice administered with sclareol.

### 3.3 | Sclareol prevents diabetes-induced inflammatory response in kidneys by inhibiting NF- $\kappa$ B and MAPKs

Our group has previously shown that NF- $\kappa$ B is activated in renal tissues of STZ-induced diabetic mice (Li et al., 2020). Studies have shown that sclareol potentially inhibits proinflammatory TNF- $\alpha$  and IL-6 secretion in murine model of rheumatoid arthritis, which is associated with NF- $\kappa$ B pathways (Tsai et al., 2018). Therefore, we wanted to confirm whether the reno-protective effects of sclareol in diabetic mice were mediated via NF- $\kappa$ B pathways-induced inflammatory responses. As shown in Figure 3a, the number of F4/80-positive and TNF- $\alpha$ -positive cells in the renal tissues of T1DM mice was markedly increased compared with the control group. Interestingly, sclareol treatment attenuated F4/80-positive macrophages and TNF- $\alpha$ -positive cells. Similarly, the mRNA levels of TNF- $\alpha$ , IL-6, and IL-1 $\beta$  in the renal tissues from T1DM mice were significantly lower than that of normal mice ( $p < 0.001$ , Figure 3b–d). In addition, mRNA levels of ICAM-1, VCAM-1, and MCP-1 were significantly elevated in the T1DM group ( $p < 0.001$ , Figure 3e–g). However, sclareol dampened diabetes-induced increases in transcript levels of inflammatory cytokines and adhesion molecules in a dose-dependent manner (Figure 3b–g). We performed a western blot experiment to detect NF- $\kappa$ B activation. As shown in Figure 3h, the I $\kappa$ B $\alpha$  was obviously degraded in vehicle group when compared to the control group. On the other hand, sclareol treatment successfully reversed the diabetes-induced degradation of I $\kappa$ B $\alpha$ , and increases of nuclear NF- $\kappa$ B p65 expression and concomitant reductions in cytosolic NF- $\kappa$ B p65 levels in a dose-dependent manner (Figure 3h). Further western blotting confirmed the remarkable upregulation of the MAPK pathway, such

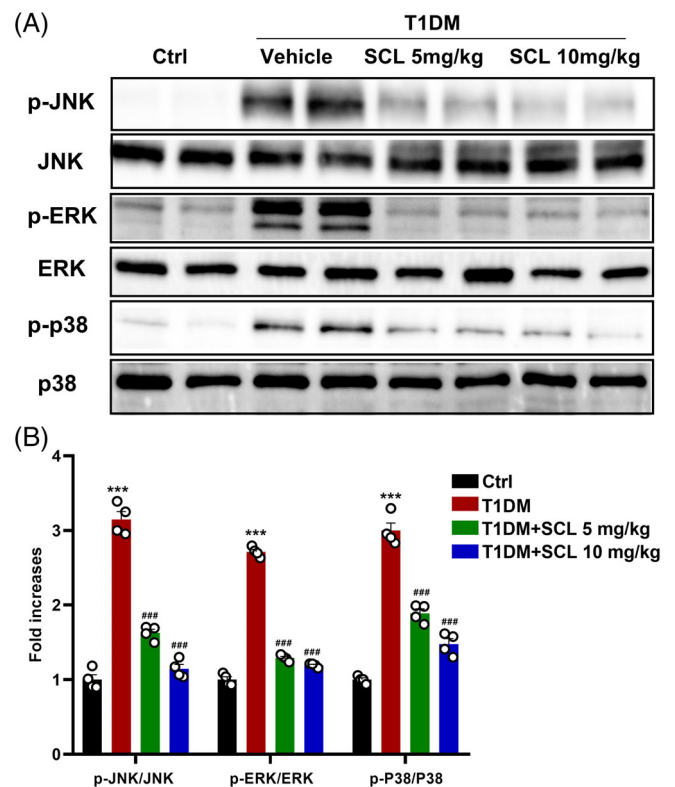


**FIGURE 4** Sclareol suppresses diabetes-induced the activation of MAPKs. (a) Western blot analysis of phosphorylated JNK, ERK, and p38 in the kidney tissues of diabetic mice, and quantitative analysis (b–d). Values are mean  $\pm$  SD, ( $n = 4$  per group). \*\*\* $p < 0.001$  versus ctrl; ### $p < 0.001$  versus T1DM. Ctrl, control; T1DM, type 1 diabetes mellitus

as increased phosphorylation of JNK, ERK, and p38 in the kidney tissues of the vehicle group compared with the control group ( $p < 0.001$ , Figure 4a–d). While these increases were completely blocked with sclareol treatment at 5 mg/kg and 10 mg/kg ( $p < 0.001$ , Figure 4a–d), these results suggest that sclareol alleviates T1DM-induced fibrosis and inflammatory reaction via suppression of activation of NF- $\kappa$ B and MAPK.

### 3.4 | Sclareol attenuates high glucose-induced increases in fibrosis and inflammatory factors in SV40 MES-13 cells

To further confirm the results from our in vivo studies, SV40 MES-13 cells stimulated with a 33 mM high glucose model were established in vitro. The SV40 MES-13 cells were exposed to increasing concentrations of sclareol and their viability was measured. As shown in Figure 5a, cell viability was significantly decreased at 50  $\mu$ M of sclareol and higher concentrations. Thus, subsequent studies were conducted with 10 and 20  $\mu$ M concentrations of sclareol, which had no significant cytotoxicity. Transcript levels of TGF- $\beta$  and Col-4 were significantly enhanced in HG-

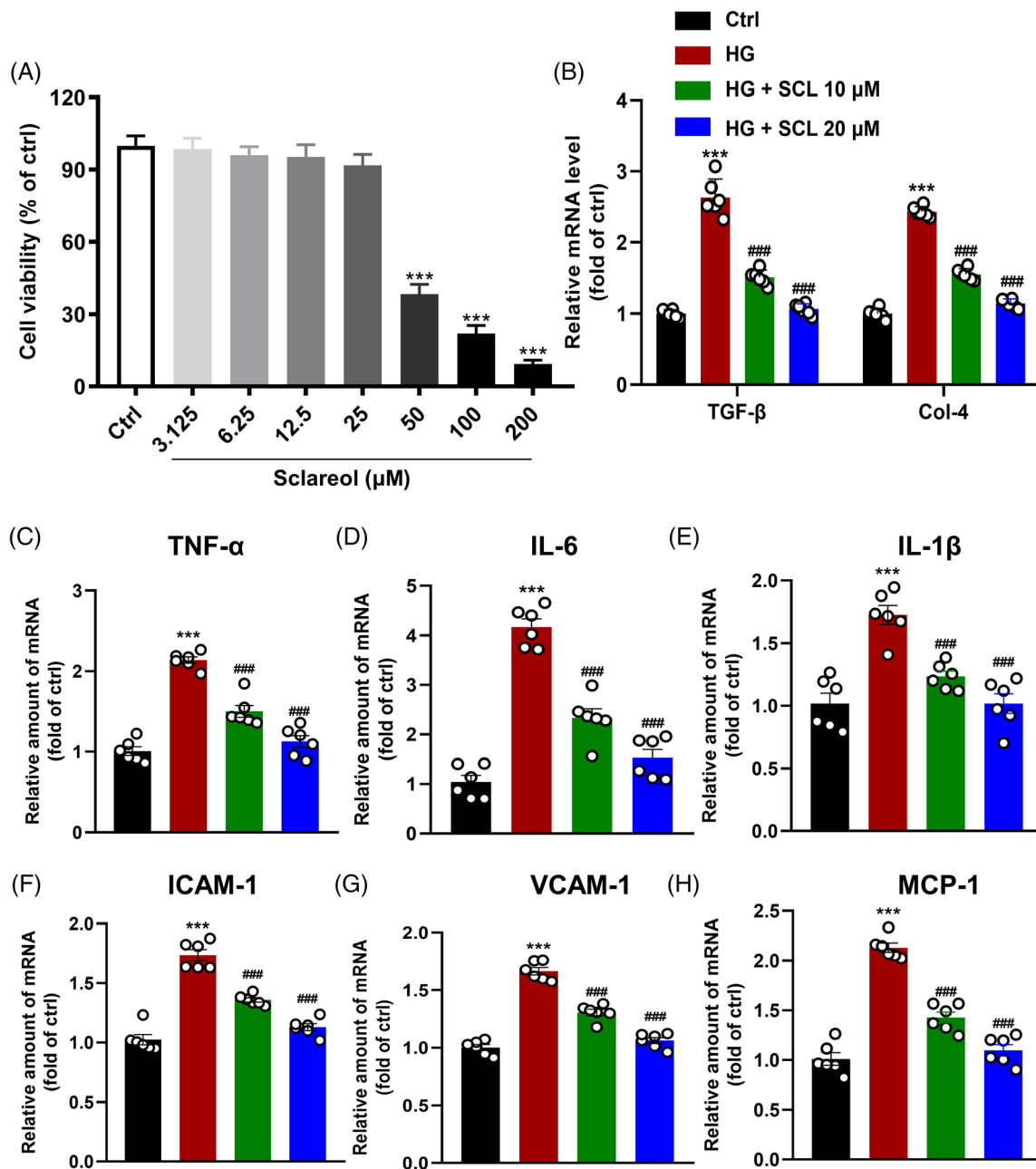


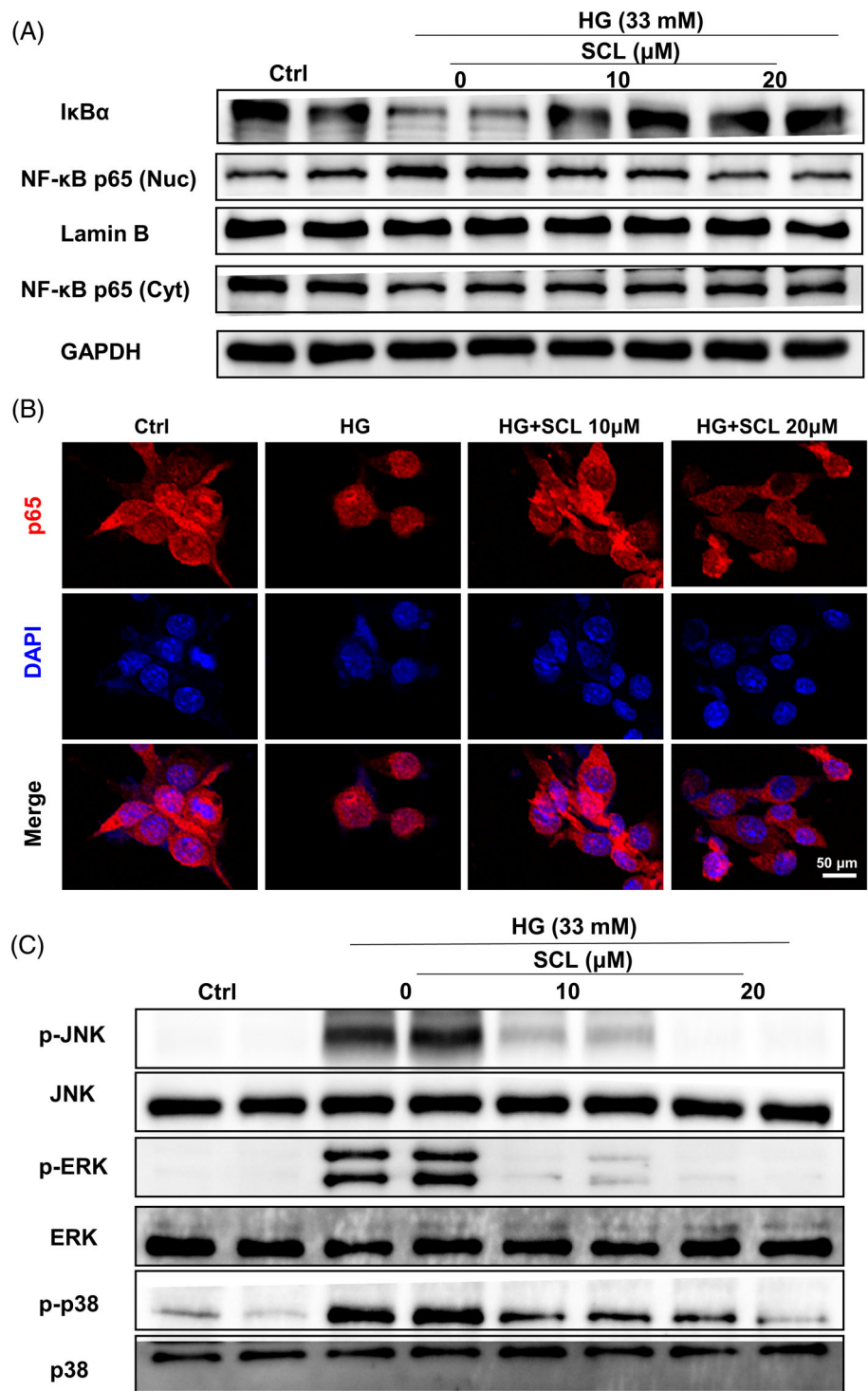
**FIGURE 5** Scclareol attenuates high glucose-induced increases of fibrosis and inflammatory factors in SV40 MES-13 cells. (a) SV40 MES-13 cells were challenged to increasing concentrations of sclareol for 24 h, and cell viability was detected with the CCK-8 assay. Transcript levels of TGF- $\beta$  and col-4 (b), TNF- $\alpha$  (c), IL-6 (d), IL-1 $\beta$  (e), ICAM-1 (f), VCAM-1 (g), and MCP-1 (h) were measured with RT-PCR in SV40 MES-13 cells. Cells were pretreated with 10 or 20  $\mu$ M sclareol for 1 hr, and then incubated with 33 mM HG for 36 h (B) or 6 hr (c-h). Values are mean  $\pm$  SD, ( $n = 6$  per group). \*\*\*  $p < 0.001$  versus ctrl; ###  $p < 0.001$  versus HG. Ctrl, control; HG, high glucose

challenged cells, while sclareol treatment obviously reduced these fibrotic factors ( $p < 0.001$ , Figure 5b). Moreover, HG increased mRNA levels of inflammatory factors including TNF- $\alpha$ , IL-6, and IL-1 $\beta$  but not in cells with sclareol treatment ( $p < 0.001$ , Figure 5c-e). In addition, sclareol treatment prevented the HG-induced increase of adhesion molecules in SV40 MES-13 cells ( $p < 0.001$ , Figure 5f-h). Our findings indicate that sclareol protects against HG-induced fibrotic factors and inflammatory cytokine production in SV40 MES-13 cells.

### 3.5 | Scclareol attenuates high glucose-induced inflammatory reactions via the MAPK-mediated NF- $\kappa$ B pathway in SV40 MES-13 cells

Next, to investigate mechanistic insights into the efficiency of sclareol in DN, we measured the protein levels of MAPKs and the NF- $\kappa$ B pathway in SV40 MES-13 cells. Scclareol treatment decreased HG-stimulated activation of NF- $\kappa$ B, evidenced by the down-regulated degradation of I $\kappa$ B $\alpha$  and the nuclear translocation of

**FIGURE 6** Sclareol attenuates high glucose-induced activations of NF- $\kappa$ B and MAPKs in SV40 MES-13 cells. SV40 MES-13 cells were pretreated with 10 or 20  $\mu$ M sclareol for 1 hr, and then incubated with 33 mM HG for 1 hr. (a) Western blot assay for measuring protein levels of NF- $\kappa$ B pathway in HG-induced SV40 MES-13 cells. (b) Representative images of immunofluorescence staining for p65 (red) and DAPI (blue). Sclareol inhibited the nuclear translocation of p65 subunit under HG condition in SV40 MES-13 cells. Scale bar, 50  $\mu$ m. (c) SV40 MES-13 cells were pretreated with 10 or 20  $\mu$ M sclareol for 1 h, and challenged with 33 mM HG for 30 min. Western blot assay was used to measure the protein expression levels of MAPKs pathway. Ctrl, control; HG, high glucose



NF- $\kappa$ B p65 subunit, as well as the upregulation of NF- $\kappa$ B p65 in the cytoplasm of SV40 MES-13 cells ( $p < 0.001$ , Figure 6a, Figure S1B). Consistent with these findings, the immunofluorescent localization of NF- $\kappa$ B showed that sclareol reduced HG-induced nuclear translocation of the p65 subunit (Figure 6b). Similarly, phosphorylation of JNK, ERK, and p38 was significantly reduced by sclareol in HG-stimulated SV40 MES-13 cells ( $p < 0.001$ , Figure 6c, Figure S1C). However, compared with the NG, SV-40 EMS-13 cells treated with mannitol (regard as the osmotic control for the HG) showed no

significant differences in expression of MAPKs and NF- $\kappa$ B pathway related proteins ( $p > 0.05$ , Figure S2). Collectively, these results indicate that sclareol inhibits HG-induced activation of NF- $\kappa$ B and MAPKs in SV40 MES-13 cells.

To determine whether or not NF- $\kappa$ B-mediated inflammatory reaction was dependent on the activation of MAPKs, we used a mixture containing a JNK inhibitor (SP00125), an ERK inhibitor (U0126), and a p38 inhibitor (SB203580) to pre-treat SV40 MES-13 cells for 30 min before sclareol treatment. The inhibition of MAPK

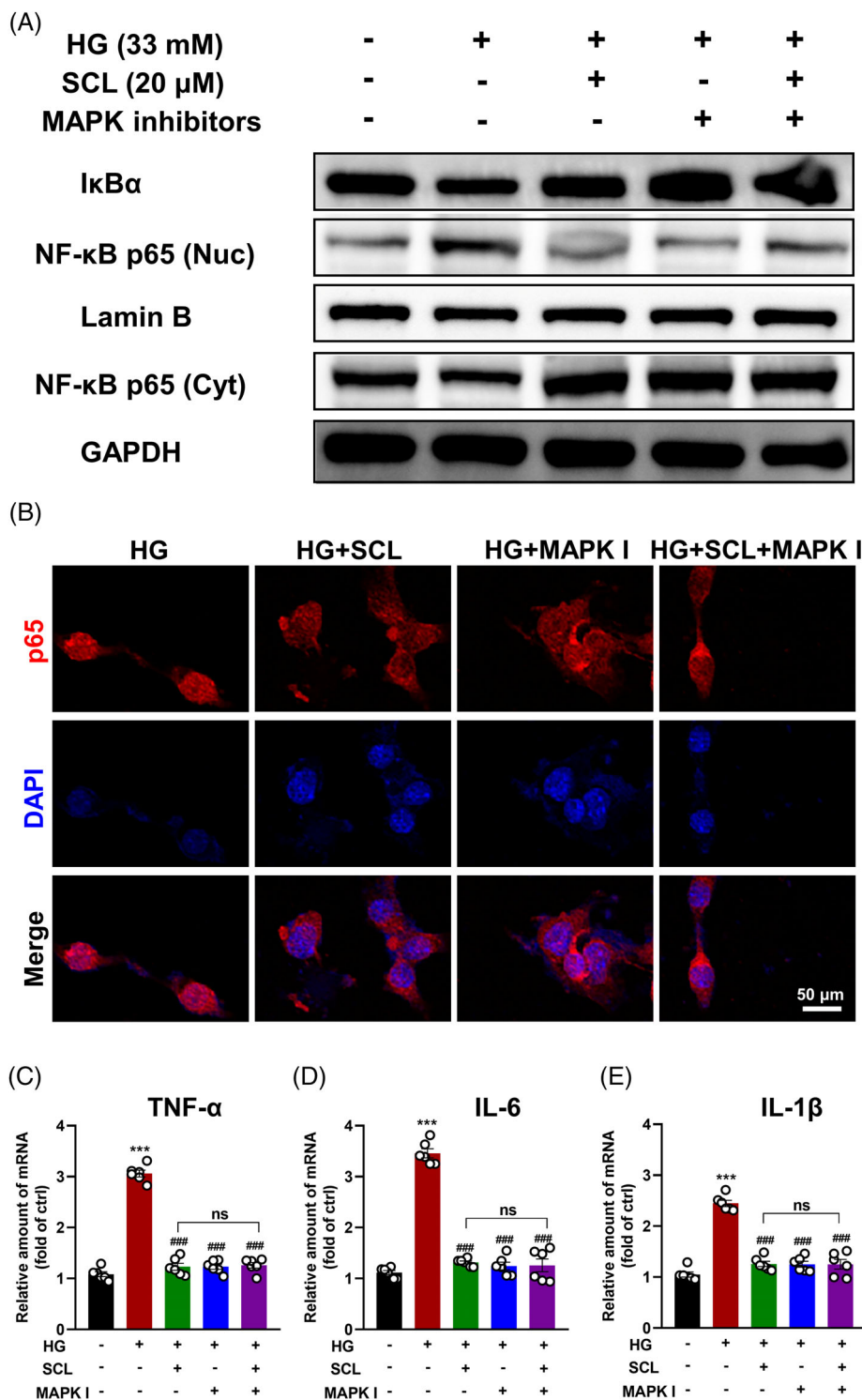
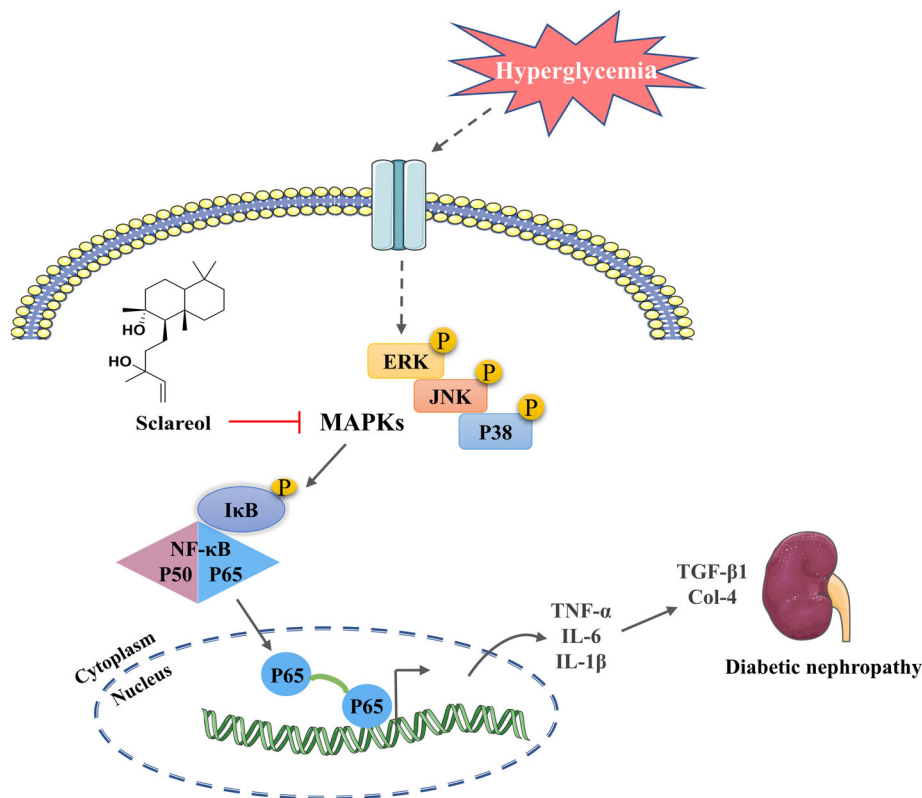


**FIGURE 7** Scloreol regulates high glucose-induced inflammatory factors through inhibiting MAPK/NF- $\kappa$ B signaling pathway in SV40 MES-13 cells. SV40 MES-13 cells were pretreated with MAPK inhibitors mixture for 1 hr, and then incubated with 20  $\mu$ M scloreol and 33 mM HG for 1 hr. (a) Protein levels of NF- $\kappa$ B pathway was measured with Western blot assay in SV40 MES-13 cells. (b) Representative images for p65 with immunofluorescence staining. MAPK inhibitors mixture also inhibited the nuclear translocation of p65 subunit in HG-induced SV40 MES-13 cells. Scale bar, 50  $\mu$ m. Transcript levels of TNF- $\alpha$  (c), IL-6 (d), and IL-1 $\beta$  (e) in SV-40 cells. Values are mean  $\pm$  SD, (a-b:  $n = 3$  per group; c-e:  $n = 6$  per group). \*\*\* $p < 0.001$  versus ctrl; ### $p < 0.001$  versus HG. Ctrl, control; HG, high glucose; ns, no significance

by the inhibitor mixture significantly suppressed the degradation of I $\kappa$ B $\alpha$  and nuclear translocation of NF- $\kappa$ B p65 subunit in HG-stimulated SV40 MES-13 cells ( $p < 0.001$ , Figure 7a, Figure S1D). As expected, there was no significant difference between the HG + MAPK inhibitors mixture and the HG + scloreol + MAPK inhibitors mixture in terms of the inhibition of NF- $\kappa$ B activation in SV40 MES-13 cells ( $p > 0.05$ , Figure 7a, Figure S1D). Immunofluorescent localization of NF- $\kappa$ B presented similar results in vitro

(Figure 7b). Furthermore, the MAPK inhibitors mixture significantly reduced HG-induced mRNA levels increase of TNF- $\alpha$ , IL-6, and IL-1 $\beta$  in SV-40 cells, while the scloreol and MAPK inhibitors mixture treatment also decreased mRNA levels of inflammatory factors ( $p < 0.001$ , Figure 7c-e). These data provide evidence that scloreol regulates inflammation under high glucose conditions via the MAPK/NF- $\kappa$ B signaling pathway. A schematic of the mechanism is displayed in Figure 8.

**FIGURE 8** The graphic illustration of the mechanism of sclareol protecting against diabetic nephropathy



## 4 | DISCUSSION

In the present study, the following key findings were obtained: (1) diabetic mice administrated with sclareol exhibited alleviated kidney dysfunction and decreased fibrosis and inflammatory responses in renal tissues in a dose-dependent manner; (2) these improvements are closely associated with the inhibition of the activation of MAPKs and NF- $\kappa$ B by sclareol *in vivo*; (3) the beneficial effects of sclareol on high glucose-induced fibrosis and inflammation in glomeruli mesangial cells were partly through the suppression of the MAPK-mediated NF- $\kappa$ B pathway *in vitro*. Taken together, we show novel clues for the therapeutic effect of sclareol on DN by improving of renal fibrosis and inflammatory responses via mediation of the MAPKs/NF- $\kappa$ B signaling pathway in type 1 diabetic mice.

DN arising from diabetes is one of the primary causes of ESRD worldwide. Clinically, BUN and urinary albumin are two important indexes for evaluating the development of DN (Tsai et al., 2018). In this study, we show that sclareol prevents upregulation of both BUN and urinary albumin to creatinine ratio in T1DM mice. However, the most corresponding and significant pathological injury identified in DN patients with renal biopsies is the occurrence of glomerular lesions, which present as diffuse mesangial expansion, glomerular basement membrane thickening, and fibrosis (Maewaza, Takemoto, & Yokote, 2015). We observed that these pathological damages were dramatically diminished by sclareol administration in the kidney tissues of diabetic mice. Interestingly, our results clearly showed that this reno-protective effect of sclareol was without any effect on the levels of blood glucose and body weight in type I diabetic mice. Thus,

the underlying mechanism for sclareol improvement of kidney dysfunction under the pathologic condition of hyperglycemia remains a huge barrier yet to be explained.

Among the various factors that could positively interact in the pathogenesis of DN, gender, hypertension, and hyperuricemia have been well studied (Donate-Correa, Martín-Núñez, Muros-de-Fuentes, Mora-Fernández, & Navarro-González, 2015; Oguiza et al., 2015). In recent years, studies have shown that the inflammation mechanism plays a central role in driving the progression of DN through diverse pro-inflammatory cytokines, such as TNF- $\alpha$ , IL-1 $\beta$ , IL-6, and MCP-1. Sclareol, as a bioactive diterpene, has been reported to possess anti-inflammation potential. Sclareol effectively inhibited the release of TNF- $\alpha$ , IL-1 $\beta$  and IL-6 in LPS-induced acute lung injury mice model (Hsieh et al., 2017). In our study, sclareol exhibited a robust anti-inflammation profile in the kidneys, reflected by downregulated mRNA levels of proinflammatory cytokines, adhesion cytokines, and F4/80-positive macrophage infiltration. Despite the advancing field, the molecular mechanism for sclareol's anti-inflammation action in diabetes is still unspecified.

The transcription factor NF- $\kappa$ B is positively correlated with renal dysfunction. It is evident that the degradation of I $\kappa$ B $\alpha$  could promote the translocation of NF- $\kappa$ B p50/p65 subunits into the nucleus and the binding of these subunits to strict promoter sequence of the aim at inflammatory genes. Several pre-clinical study and clinical study studies have reported that NF- $\kappa$ B activation plays a key role in the pathogenesis of DN inflammation and fibrosis (Jiang, Liu, Zhou, Liu, & Liu, 2020; Yang et al., 2021). Our previous studies have found that inhibition of the activation of NF- $\kappa$ B contributes to attenuating the

renal inflammation and fibrosis in both type 1 diabetes and type 2 diabetes (Li et al., 2020; Yang et al., 2021). Moreover, Sclareol has been reported to inhibit the breakdown of NF- $\kappa$ B and the phosphorylation of MAPKs in lung tissues (Hsieh et al., 2017). In this study, we confirmed that sclareol suppressed the nuclear translocation of NF- $\kappa$ B and the degradation of I $\kappa$ B $\alpha$  both in kidney tissues and in HG-induced SV40 MES-13 cells. Our data suggest that the anti-inflammation activation of sclareol is strongly associated with the transcriptional suppression of the NF- $\kappa$ B pathway.

MAPK families (JNK, ERK, and p38) which are important players in the signal transduction pathway, contribute to boosting the production of cytokines (Liang et al., 2018). The MAPK signaling pathway is activated by the phosphorylation of JNK, ERK, and p38 in response to various stimuli including hyperglycemia, and mediates its function by downstream of inflammation (Li et al., 2021). Our data provided evidences that not only renal tissues from T1DM mice presented with phosphorylated MAPKs, but HG activated MAPKs in mesangial cells as well, and sclareol downregulated MAPKs phosphorylation in both of these cases. In addition, NF- $\kappa$ B has been reported to be activated by MAPK to induce chronic inflammation in DN (Malik et al., 2017). In our experimental model, we wondered if the NF- $\kappa$ B activation resulted from JNK, ERK, and p38 activation. We observed that the JNK, ERK, and p38 inhibitors mixture prevented HG-induced nuclear translocation of NF- $\kappa$ B, and decreased HG-stimulated elevation of inflammatory cytokines in SV40 MES-13 cells. Consequently, our data suggest that the anti-inflammation action of sclareol may be via suppression of the JNK, ERK, and p38 pathways to inhibit NF- $\kappa$ B.

Actually, this study has several limitations. We did not use a positive control for evaluation the reno-protective effects on DN. Our previous study found that MD2/TLR4 complex could trigger the activation of MAPKs under HG condition in kidneys (Wang et al., 2019). It suggests that MD2/TLR4 may be the up-stream pathway of MAPKs in diabetic condition. However, in this study, the specific up-stream pathway of MAPKs regulated by sclareol need further study.

## 5 | CONCLUSION

In summary, we show that sclareol possibly protects against diabetic nephropathy in T1DM mice. Sclareol has promising and broad anti-inflammation action, inhibiting cytokine production, F4/80-positive macrophage infiltration, induction of adhesion factors, and the activation of MAPKs and the NF- $\kappa$ B pathway in diabetic kidneys. In correspondence with its reno-protective effects, sclareol prevented HG-induced inflammation via MAPKs/NF- $\kappa$ B pathways in vitro. Our study may provide insights into new applications of sclareol to alleviate renal damage in diabetic individuals.

## ACKNOWLEDGMENTS

This study was supported by the National Natural Science Foundation of China (31900381 to X.H. and 21961142009 to G.L.), Zhejiang Provincial Key Scientific Project (2021C03041 to G.L.), the Natural Science Foundation of Zhejiang Province (LGJ18H310002 to X.H.), and

Wenzhou Science and Technology Key Project (2018ZY009 to G.L.), and the Basic Scientific Research Project of Hangzhou Medical College (KYZD202102 to Q.J.S. and KYB202114 to X.H.).

## AUTHOR CONTRIBUTIONS

Guang Liang, Huazhong Ying, and Yi Wang contributed to the literature search and study design. Xue Han, Yi Zhang, and Huazhong Ying participated in the drafting of the article. Xue Han, Jijia Zhang, Li Zhou, Jijia Wei, Yu Tu, Qiaojuan Shi, and Juan Ren carried out the experiments. Yi Wang and Guang Liang revised the manuscript. Xue Han and Huazhong Ying contributed to data collection and analysis.

## CONFLICTS OF INTEREST

The authors declare that they have no conflict of interest.

## ORCID

Guang Liang  <https://orcid.org/0000-0002-8278-849X>

## REFERENCES

- Cerri, G. C., Lima, L. C. F., Lelis, D. F., Barcelos, L. D. S., Feltenberger, J. D., Mussi, S. V., ... Santos, S. H. S. (2019). Sclareol-loaded lipid nanoparticles improved metabolic profile in obese mice. *Life Sciences*, 218, 292–299. <https://doi.org/10.1016/j.lfs.2018.12.063>
- Donate-Correa, J., Martín-Núñez, E., Muros-de-Fuentes, M., Mora-Fernández, C., & Navarro-González, J. F. (2015). Inflammatory cytokines in diabetic nephropathy. *Journal Diabetes Research*, 2015, 948417. <https://doi.org/10.1155/2015/948417>
- Duan, G., Hou, S., Ji, J., & Deng, B. (2018). The study of sclareol in inhibiting proliferation of osteosarcoma cells by apoptotic induction and loss of mitochondrial membrane potential. *Cancer Biomarkers*, 22(1), 29–34. <https://doi.org/10.3233/cbm-170698>
- Fioretto, P., Zambon, A., Rossato, M., Busetto, L., & Vettor, R. (2016). SGLT2 inhibitors and the diabetic kidney. *Diabetes Care*, 39(Suppl. 2), S165–S171.
- Hsieh, Y. H., Deng, J. S., Pan, H. P., Liao, J. C., Huang, S. S., & Huang, G. J. (2017). Sclareol ameliorate lipopolysaccharide-induced acute lung injury through inhibition of MAPK and induction of HO-1 signaling. *International Immunopharmacology*, 44, 16–25. <https://doi.org/10.1016/j.intimp.2016.12.026>
- Jaimes, E. A., Zhou, M. S., Siddiqui, M., Rezonzew, G., Tian, R., Seshan, S. V., ... Raji, L. (2021). Nicotine, smoking, podocytes, and diabetic nephropathy. *American Journal of Physiology. Renal Physiology*, 320(3), F442–f453. <https://doi.org/10.1152/ajprenal.00194.2020>
- Jiang, Y., Liu, J., Zhou, Z., Liu, K., & Liu, C. (2020). Fangchinoline protects against renal injury in diabetic nephropathy by modulating the MAPK signaling pathway. *Experimental and Clinical Endocrinology & Diabetes*, 128(8), 499–505. <https://doi.org/10.1055/a-0636-3883>
- Jiao, Z., Chen, J., Liu, Y., Liu, T., Chen, K., & Li, G. (2015). Role of ERK1/2 and JNK phosphorylation in iodine contrast agent-induced apoptosis in diabetic rat kidneys. *Renal Failure*, 37(8), 1349–1355. <https://doi.org/10.3109/0886022x.2015.1068031>
- Jin, H., Shao, Z., Wang, Q., Miao, J., Bai, X., Liu, Q., ... Xu, J. (2019). Sclareol prevents ovariectomy-induced bone loss in vivo and inhibits osteoclastogenesis in vitro via suppressing NF- $\kappa$ B and MAPK/ERK signaling pathways. *Food & Function*, 10(10), 6556–6567. <https://doi.org/10.1039/c9fo00206e>
- Kale, A., Sankrityayan, H., Anders, H. J., & Gaikwad, A. B. (2021). Epigenetic and non-epigenetic regulation of klotho in kidney disease. *Life Sciences*, 264, 118644. <https://doi.org/10.1016/j.lfs.2020.118644>

- Kang, H. H., Kim, I. K., Lee, H. I., Joo, H., Lim, J. U., Lee, J., ... Moon, H. S. (2017). Chronic intermittent hypoxia induces liver fibrosis in mice with diet-induced obesity via TLR4/MyD88/MAPK/NF- $\kappa$ B signaling pathways. *Biochemical and Biophysical Research Communications*, 490(2), 349–355. <https://doi.org/10.1016/j.bbrc.2017.06.047>
- Kumar, S., Mittal, A., Babu, D., & Mittal, A. (2021). Herbal medicines for diabetes management and its secondary complications. *Current Diabetes Reviews*, 17(4), 437–456. <https://doi.org/10.2174/1573399816666201103143225>
- Li, L., Ding, C., Zou, C., Xiong, Z., Zhu, W., Qian, J., ... Liang, G. (2020). A novel salvianone derivative, compound 15a, attenuates diabetes-induced renal injury by inhibiting NF- $\kappa$ B-mediated inflammatory responses. *Toxicology and Applied Pharmacology*, 409, 115322. <https://doi.org/10.1016/j.taap.2020.115322>
- Li, Y., Hou, J. G., Liu, Z., Gong, X. J., Hu, J. N., Wang, Y. P., ... Li, W. (2021). Alleviative effects of 20(R)-Rg3 on HFD/STZ-induced diabetic nephropathy via MAPK/NF- $\kappa$ B signaling pathways in C57BL/6 mice. *Journal of Ethnopharmacology*, 267, 113500. <https://doi.org/10.1016/j.jep.2020.113500>
- Liang, G., Song, L., Chen, Z., Qian, Y., Xie, J., Zhao, L., ... Huang, Z. (2018). Fibroblast growth factor 1 ameliorates diabetic nephropathy by an anti-inflammatory mechanism. *Kidney International*, 93(1), 95–109. <https://doi.org/10.1016/j.kint.2017.05.013>
- Maezawa, Y., Takemoto, M., & Yokote, K. (2015). Cell biology of diabetic nephropathy: Roles of endothelial cells, tubulointerstitial cells and podocytes. *Journal of Diabetes Investigation*, 6(1), 3–15. <https://doi.org/10.1111/jdi.12255>
- Malik, S., Suchal, K., Khan, S. I., Bhatia, J., Kishore, K., Dinda, A. K., & Arya, D. S. (2017). Apigenin ameliorates streptozotocin-induced diabetic nephropathy in rats via MAPK-NF- $\kappa$ B-TNF- $\alpha$  and TGF- $\beta$ 1-MAPK-fibronectin pathways. *American Journal of Physiology. Renal Physiology*, 313(2), F414–f422. <https://doi.org/10.1152/ajprenal.00393.2016>
- Mozzini, C., Cominacini, L., Garbin, U., & Fratta Pasini, A. M. (2017). Endoplasmic reticulum stress, NRF2 Signalling and cardiovascular diseases in a nutshell. *Current Atherosclerosis Reports*, 19(8), 33. <https://doi.org/10.1007/s11883-017-0669-7>
- Oguiza, A., Recio, C., Lazaro, I., Mallavia, B., Blanco, J., Egido, J., & Gomez-Guerrero, C. (2015). Peptide-based inhibition of I $\kappa$ B kinase/nuclear factor- $\kappa$ B pathway protects against diabetes-associated nephropathy and atherosclerosis in a mouse model of type 1 diabetes. *Diabetologia*, 58(7), 1656–1667. <https://doi.org/10.1007/s00125-015-3596-6>
- Patel, D. M., Bose, M., & Cooper, M. E. (2020). Glucose and blood pressure-dependent pathways—the progression of diabetic kidney disease. *International Journal of Molecular Sciences*, 21(6), 2218. <https://doi.org/10.3390/ijms21062218>
- Ravera, S., Esposito, A., Degan, P., Caicci, F., Calzia, D., Perrotta, E., ... Panfoli, I. (2020). Sclereol modulates free radical production in the retinal rod outer segment by inhibiting the ectopic f(1)f(o)-atp synthase. *Free Radical Biology & Medicine*, 160, 368–375. <https://doi.org/10.1016/j.freeradbiomed.2020.08.014>
- Tsai, S. W., Hsieh, M. C., Li, S., Lin, S. C., Wang, S. P., Lehman, C. W., ... Lin, C. C. (2018). Therapeutic potential of Sclereol in experimental models of rheumatoid arthritis. *International Journal of Molecular Sciences*, 19(5), 1351. <https://doi.org/10.3390/ijms19051351>
- Varma, V. K., Kajdacsy-Balla, A., Akkina, S. K., Setty, S., & Walsh, M. J. (2016). A label-free approach by infrared spectroscopic imaging for interrogating the biochemistry of diabetic nephropathy progression. *Kidney International*, 89(5), 1153–1159. <https://doi.org/10.1016/j.kint.2015.11.027>
- Vleming, L. J., Baelde, J. J., Westendorp, R. G., Daha, M. R., van Es, L. A., & Bruijn, J. A. (1997). The glomerular deposition of PAS positive material correlates with renal function in human kidney diseases. *Clinical Nephrology*, 47(3), 158–167.
- Wada, J., & Makino, H. (2013). Inflammation and the pathogenesis of diabetic nephropathy. *Clinical Science*, 124(3), 139–152. <https://doi.org/10.1042/cs20120198>
- Wang, Y., Fang, Q. L., Jin, Y. Y., Liu, Z. D., Zou, C. P., Yu, W. H., ... Liang, G. (2019). Blockade of myeloid differentiation 2 attenuates diabetic nephropathy by reducing activation of the renin-angiotensin system in mouse kidneys. *British Journal of Pharmacology*, 176(14), 2642–2657. <https://doi.org/10.1111/bph.14687>
- Wang, Y., Luo, W., Han, J. B., Khan, Z. A., Fang, Q. L., Jin, Y. Y., ... Liang, G. (2020). MD2 activation by direct AGE interaction drives inflammatory diabetic cardiomyopathy. *Nature Communications*, 11(1), 2148. <https://doi.org/10.1038/s41467-020-15978-3>
- Yang, C., Chen, X. C., Li, Z. H., Wu, H. L., Jing, K. P., Huang, X. R., ... Liu, H. F. (2021). SMAD3 promotes autophagy dysregulation by triggering lysosome depletion in tubular epithelial cells in diabetic nephropathy. *Autophagy*, 17(9), 2325–2344. <https://doi.org/10.1080/15548627.2020.1824694>
- Yang, X., Luo, W., Li, L., Hu, X., Xu, M., Wang, Y., ... Liang, G. (2021). CDK9 inhibition improves diabetic nephropathy by reducing inflammation in the kidneys. *Toxicology and Applied Pharmacology*, 416, 115465. <https://doi.org/10.1016/j.taap.2021.115465>
- Zhang, T., Wang, T., & Cai, P. (2017). Sclereol inhibits cell proliferation and sensitizes cells to the antiproliferative effect of bortezomib via upregulating the tumor suppressor caveolin-1 in cervical cancer cells. *Molecular Medicine Reports*, 15(6), 3566–3574. <https://doi.org/10.3892/mmr.2017.6480>

## SUPPORTING INFORMATION

Additional supporting information may be found in the online version of the article at the publisher's website.

**How to cite this article:** Han, X., Zhang, J., Zhou, L., Wei, J., Tu, Y., Shi, Q., Zhang, Y., Ren, J., Wang, Y., Ying, H., & Liang, G. (2022). Sclereol ameliorates hyperglycemia-induced renal injury through inhibiting the MAPK/NF- $\kappa$ B signaling pathway. *Phytotherapy Research*, 36(6), 2511–2523. <https://doi.org/10.1002/ptr.7465>